

In-medium pion dispersion relation, $N\pi \rightarrow \Delta$ cross section and $\Delta \rightarrow N\pi$ decay width in asymmetric nuclear matter

Ying Cui,^{1,*} Yingxun Zhang,^{1,2,†} and Zhuxia Li¹

¹*China Institute of Atomic Energy, Beijing 102413, China*

²*Guangxi Key Laboratory Breeding Base of Nuclear Physics and Technology,
Guangxi Normal University, Guilin 541004, China*

(Dated: May 31, 2022)

The pion dispersion relation, in-medium $N\pi \rightarrow \Delta$ cross section and $\Delta \rightarrow N\pi$ decay width are investigated in isospin asymmetric nuclear matter by using the same relativistic interaction within the framework of one-boson-exchange model. With the consideration of the energy conservation effect, the in-medium $N\pi \rightarrow \Delta$ cross sections are reduced near the low energy ($s^{1/2} < 1.25$ GeV) and enhanced in the high energy region ($s^{1/2} > 1.25$ GeV) in symmetric nuclear matter. The in-medium correction factors are different for different channels in asymmetric nuclear matter. It could result a higher pion multiplicity and higher π^-/π^+ ratios in the transport model simulations than the calculations without considering the in-medium effects, if other terms remain unchanged. Our study hints a systematically study on the pion production mechanism in heavy ion collisions are urged and it could be useful for understanding the in-medium effects of pions.

I. INTRODUCTION

The symmetry energy plays an important role for understanding the isospin asymmetric subject, such as neutron stars [1, 2] and the neutron rich heavy ion collisions observables [3–5], but the density dependence of symmetry energy, especially at high density, is still in uncertainties. Even there are some efforts on the constraints of the symmetry energy at suprasaturation density by analyzing the neutron star merging events [2, 6–15], the constraints from the heavy ion collisions are also needed. The ratio of multiplicity of π^- to π^+ , simply named as π^-/π^+ ratios, in heavy ion collisions with neutron rich beam and target at the beam energy of Δ threshold energy was supposed to be a sensitive observable to probe the density dependence of the symmetry energy at suprasaturation density [16].

The pion data of Au+Au at the beam energy ranging from 0.4 GeV/nucleon to 1.2 GeV/nucleon [17] have been used for extracting the symmetry energy, however, the contradictory conclusions on the symmetry energy have been obtained by comparing the data to the calculations with different transport models [18–23]. Besides the model uncertainties which comes from the philosophy of solving the high dimensionality transport equation, another important reason is that the sensitivity of π^-/π^+ ratios may be not so strong to distinguish the stiffness of symmetry energy very clear at higher beam energy where the nucleon-nucleon collisions play the dominant roles instead of the mean field. It stimulates the remeasurement of pion multiplicities and π^-/π^+ ratios near the Δ threshold energy or at subthreshold energy by using neutron rich reaction systems.

Very recently, MSU group measured the charged pion multiplicities for $^{132,112,108}\text{Sn} + ^{124,112}\text{Sn}$ by using the S π RIT Time Projection Chamer at 270 MeV/nucleon, which is subthreshold energy. The energy spectral of single π^-/π^+ ratios, i.e., $R(\pi^-/\pi^+) = \frac{dM_{\pi^-}}{dE_k} / \frac{dM_{\pi^+}}{dE_k}$, and double ratios $DR(\pi^-/\pi^+) = R_2(\pi^-/\pi^+)/R_1(\pi^-/\pi^+)$ will be provided, and they may have a more exclusive sensitivity to the density dependence of the symmetry energy than the total multiplicity of pions [21, 24].

However, the behavior of the pion energy spectral or pion flow could also be sensitive to the pion potential [25–29]. The reason is that, near the beam energy around 300 MeV/nucleon, the pions are produced through the low mass Δ s. The produced pions via the low mass Δ s decay have the smaller momentum, so they have the longer mean-free-path since the cross sections of $\pi + N$ near the threshold energies are relative small [30]. Consequently, one can expect that the in-medium effects on pion propagation and collision become more and more important. The relativistic Vlasov-Uehling-Uhlenbeck (RVUU) model calculations had shown that the π^-/π^+ ratio is reduced about 10% by considering the in-medium pion dispersion relation, and a large effect is also observed in isospin-dependent Boltzmann-Uehling-Uhlenbeck (IBUU) [27] calculations at subthreshold energy. There exists the model dependence on the in-medium effects on the pion production mechanism in the transport model simulations partly due to the separate treatments on pion potential, the $\pi N \rightarrow \Delta$ cross sections and $\Delta \rightarrow \pi N$ decay widths. Thus, providing a theoretical description on the pion potential, the $\pi N \rightarrow \Delta$ cross sections and $\Delta \rightarrow \pi N$ decay widths in isospin asymmetric nuclear matter from the same Lagrange will be very useful for us to deeply understand the pion production mechanism and reduce the model uncertainties related to the medium corrections separately for pion potential and $N\pi \rightarrow \Delta/\Delta \rightarrow N\pi$.

Generally, the pion potential can be obtained from the

*Electronic address: yingcuid@163.com

†Electronic address: zhyx@ciae.ac.cn

phenomenological pion potential [23, 26–29], or from the effective methods, such as closed-time path green functions method [31], chiral perturbation theory [32, 33]. Dmitriev el at. did the study on the in-medium pion dispersion relation by the pion self-energy via meson exchange interaction [34] for symmetric nuclear matter. After that, the work from Guangjun Mao had also given the discussion about the pion dispersion relation with the relativistic form of pion self-energy in symmetric nuclear matter and its effect on the $N\pi \rightarrow \Delta$ cross section and $\Delta \rightarrow N\pi$ decay width [31, 35].

As the increasing of interests on the study of isospin asymmetric nuclear matter, Kaiser el at. had given the pion s-wave self-energy in isospin asymmetric nuclear matter based on chiral perturbation theory up to the two-loop approximation [32]. With the s-wave pion self-energy from Ref. [32], Zhang el at. also added p-wave pion potential in estimation on the in-medium $N\pi \rightarrow \Delta$ cross section and $\Delta \rightarrow \pi N$ decay width by including N and Δ masses in free space [36]. Qingfeng Li et al. had also given the discussions about the $N\pi \rightarrow \Delta$ cross section and $\Delta \rightarrow \pi N$ decay width in asymmetric nuclear matter based on the closed-time path green function methods [35], but the pion dispersion relation they used is still in symmetric nuclear matter [31]. Among those calculations, the energy conservation is an important issue and should be carefully considered in isospin asymmetric nuclear matter as for $NN \rightarrow N\Delta$ [37].

In this paper, we will investigate the pion self-energy, in-medium $N\pi \rightarrow \Delta$ cross section and $\Delta \rightarrow N\pi$ decay width with relativistic form interaction in asymmetric nuclear matter, with the consideration of the energy conservation and effective mass splitting effects. It is organized as follows. In Sec. II, we will introduce the theoretical model on the pion self-energy, $N\pi \rightarrow \Delta$ cross section and Δ decay width. Then, the in-medium pion dispersion relation, $N\pi \rightarrow \Delta$ cross section and $\Delta \rightarrow \pi N$ decay width are presented and discussed in Sec. III. Finally, the summary and conclusion are given in Sec. IV.

II. THEORETICAL MODEL

We perform the study on the in-medium pion dispersion relation based on the particle-hole and Δ -hole with relativistic form interaction, and also do the calculation the $\pi N \rightarrow \Delta$ cross sections and $\Delta \rightarrow \pi N$ decay widths in asymmetric medium. The Lagrangian we adopted as follows [37–41]

$$\mathcal{L} = \mathcal{L}_F + \mathcal{L}_I \quad (1)$$

where the \mathcal{L}_F is the free lagrangian for the nucleon and Δ [37, 41]. The interaction part of the Lagrangian is

$$\mathcal{L}_I = \frac{g_{\pi NN}}{m_\pi} \bar{\Psi} \gamma_\mu \gamma_5 \boldsymbol{\tau} \cdot \Psi \partial^\mu \boldsymbol{\pi} + \frac{g_{\pi N\Delta}}{m_\pi} \bar{\Delta}_\mu \boldsymbol{\mathcal{T}} \cdot \Psi \partial^\mu \boldsymbol{\pi} + h.c. \quad (2)$$

Here $\boldsymbol{\tau}$ is the isospin matrices of the nucleon [38], and $\boldsymbol{\mathcal{T}}$ is the isospin transition matrix between the isospin 1/2 and 3/2 fields [40].

The pion dispersion relation in nuclear medium is:

$$\omega_{\pi^i}^2 = m_{\pi^i}^2 + \mathbf{k}^2 + \Pi(k). \quad (3)$$

where π^i presents different isospin state of the pion, i.e., π^+ , π^0 , and π^- . Here, $\Pi(k)$ is the pion self-energy, it includes the particle-hole ($\Pi_N(k)$) and Δ -hole parts($\Pi_\Delta(k)$), i.e.,

$$\Pi(k) = \Pi_N(k) + \Pi_\Delta(k). \quad (4)$$

For the on-shell pion dispersion relation in Eq. (3), the $\Pi(k)$ should be the real part ($\text{Re}\Pi(k)$). For convenience, all the Re notions in the $\Pi(k)$ are ignored in this paper. The lowest order π self-energy in nuclear matter are,

$$\begin{aligned} \Pi_N = & (-i) \left(\frac{g_{\pi NN}}{m_\pi} \right)^2 \langle t' | \tau^\lambda | t \rangle \langle t | \tau^{\lambda'} | t' \rangle \delta_{\lambda\lambda'} \\ & \times \int \frac{d^4 q}{(2\pi)^4} \text{Tr}[\not{k} \gamma_5 G_N(q+k) \not{k} \gamma_5 G_N(q)], \end{aligned} \quad (5)$$

$$\begin{aligned} \Pi_\Delta = & (-i) \left(\frac{g_{\pi N\Delta}}{m_\pi} \right)^2 \langle t' | \mathcal{T}^\lambda | t \rangle \langle t | \mathcal{T}^{\lambda'} | t' \rangle \delta_{\lambda\lambda'} \\ & \times \int \frac{d^4 q}{(2\pi)^4} \text{Tr}[\not{k}_\mu \not{k}_\nu G_\Delta^{\mu\nu}(q+k) G_N(q)], \end{aligned} \quad (6)$$

where isospin matrix τ^λ can be τ^+ , τ^0 and τ^- as in Ref. [42]. Here we take the isospin factors $\langle t' | \tau^\lambda | t \rangle = I_{NN}$, and $\langle t' | \mathcal{T}^\lambda | t \rangle = I_{N\Delta}$, which can be found in the appendix B.

The nucleon and Δ propagator in nuclear medium can be written from above Lagrangian,

$$\begin{aligned} G_N(q_0, \mathbf{q}) = & \frac{\not{q} + m_N}{q_0^2 - E_N^2(q) + i\epsilon} \\ & + i2\pi \frac{\not{q} + m_N}{2E_N(q)} \theta(q_F - |\mathbf{q}|) \delta(q_0 - E_N(q)) \end{aligned} \quad (7)$$

$$\begin{aligned} G_\Delta^{\mu\nu}(q_0, \mathbf{q}) = & \frac{\mathcal{P}^{\mu\nu}}{q_0^2 - E_\Delta^2(q) + i\epsilon} \\ & + i2\pi \frac{\not{q} + m_{0,\Delta}}{2E_\Delta(q)} \theta(q_F - |\mathbf{q}|) \delta(q_0 - E_\Delta(q)) \end{aligned} \quad (8)$$

where $\mathcal{P}^{\mu\nu}$ is:

$$\mathcal{P}^{\mu\nu} = -(\not{q} + m_{0,\Delta}) [g^{\mu\nu} - \frac{1}{3} \gamma^\mu \gamma^\nu - \frac{2q^\mu q^\nu}{3m_{0,\Delta}^2} + \frac{q^\mu \gamma^\nu - q^\nu \gamma^\mu}{3m_{0,\Delta}}]. \quad (9)$$

Here, $\not{q} = q^\mu \gamma_\mu$ and $m_{0,\Delta}$ is the pole mass of Δ . The first parts of Eq. (7) - (8) are the vacuum propagators, and $\theta(q_F - |\mathbf{q}|)$ denotes the occupation number in the medium with the Fermi momentum q_F . The pion self-energies can be expressed in terms of an analog of the susceptibility χ ,

$$\Pi_N = k^2 \chi_N \quad (10)$$

$$\Pi_\Delta = k^2 \chi_\Delta \quad (11)$$

and the short range correlations is incorporated into χ as follows,

$$\begin{aligned}\chi_N &\rightarrow \frac{1 + (g'_{N\Delta} - g'_{\Delta\Delta})\chi_\Delta}{(1 - g'_{\Delta\Delta}\chi_\Delta)(1 - g'_{NN}\chi_N) - g'_{N\Delta}\chi_\Delta g'_{N\Delta}\chi_N}\chi_N, \\ \chi_\Delta &\rightarrow \frac{1 + (g'_{N\Delta} - g'_{NN})\chi_N}{(1 - g'_{\Delta\Delta}\chi_\Delta)(1 - g'_{NN}\chi_N) - g'_{N\Delta}\chi_\Delta g'_{N\Delta}\chi_N}\chi_\Delta.\end{aligned}$$

The Migdal parameters for the short-range interaction $g'_{NN} = 0.9$, $g'_{N\Delta} = g'_{\Delta\Delta} = 0.6$ as Ref. [43]. The detailed calculation and the self-energy of π^+ , π^0 and π^- are shown in the appendix B - C.

For the calculation of the in-medium $\Delta \rightarrow N\pi$ decay width and $\pi N \rightarrow \Delta$ cross section, we use the quasiparticle approximation [44] by the replacing $m_i \rightarrow m_i^*$ and $p_i \rightarrow p_i^*$ (i could be nucleon or Δ) in their formula. The effective momentum can be written as $\mathbf{p}_i^* = \mathbf{p}_i$ since the spatial components of vector field vanish in the rest nuclear matter, i.e., $\Sigma = 0$. Thus, in the mean field approach, the effective energy reads

$$p_i^{*0} = p_i^0 - \Sigma_i^0. \quad (12)$$

The Dirac effective mass of nucleon and effective pole mass of Δ read

$$m_i^* = m_i + \Sigma_i^S, \quad (13)$$

here the details about Σ_i^0 and Σ_i^S can be found in Refs. [37, 41]. And the parameters of the relativistic mean field is from the $N\Lambda\rho\delta$ in Ref. [45].

Based on the approximation we adopted, $\mathbf{p}_N + \mathbf{k} = \mathbf{p}_N^* + \mathbf{k}^*$. The energy conservation is canonical momentum conserved, i.e., $E_\Delta = E_N + \omega$, with $E_\Delta = E_\Delta^* + \Sigma_\Delta^0$, $E_N = E_N^* + \Sigma_N^0$,

$$m_\Delta^* + \Sigma_\Delta^0 = E_N^* + \Sigma_N^0 + \omega(\mathbf{k}). \quad (14)$$

By using the effective momentum and masses, one can get the in-medium $\Delta \rightarrow N\pi$ decay width and $\pi N \rightarrow \Delta$ cross section. The in-medium decay width of $\Delta \rightarrow N\pi$ is:

$$\begin{aligned}\Gamma^* &= \frac{1}{2m_\Delta^*} \int \frac{d^3\mathbf{p}_N^*}{(2\pi)^3 2E_N^*} \frac{d^3\mathbf{p}_\pi^* d\omega}{(2\pi)^3} \overline{|\mathcal{M}_{\Delta \rightarrow N\pi}|^2} \\ &\quad \times \delta(\omega^2 - \mathbf{p}_\pi^{*2} - m_\pi^2 - \Pi) \\ &\quad \times (2\pi)^4 \delta^3(\mathbf{p}_N^* + \mathbf{p}_\pi^*) \delta(E_N^* + \omega + \Delta\Sigma - m_\Delta^*) \\ &= Z_B \frac{\mathbf{k}^2}{8\pi m_\Delta^* E_N^* \omega} \frac{\overline{|\mathcal{M}_{\Delta \rightarrow N\pi}|^2}}{|\frac{\mathbf{k}}{E_N^*} + \frac{\mathbf{k}}{\omega}|} \quad (15)\end{aligned}$$

where $\mathbf{p}_\pi^* = \mathbf{p}_\pi = \mathbf{k}$ in the static nuclear medium, $\Delta\Sigma = \Sigma_N^0 - \Sigma_\Delta^0$. And the Z_B is the wave function renormalization factor,

$$Z_B = \frac{1}{1 - \frac{1}{2\omega} \frac{\partial\Pi(\omega, \mathbf{k})}{\partial\omega}|_{\omega=E_\pi^*}}, \quad (16)$$

where

$$E_\pi^* = \sqrt{\mathbf{k}^2 + m_\pi^2 + \Pi(\omega, \mathbf{k})}. \quad (17)$$

Since we focused on the cross sections which will be used near the threshold energy heavy ion collisions where the low mass Δ s dominate, the pion branch plays the main role for the Δ and the Δ -hole branch is ignored. Thus, we take $Z_B = 1$ as Ref. [31]

The in-medium $\pi N \rightarrow \Delta$ cross section is:

$$\begin{aligned}\sigma_{\pi N \rightarrow \Delta}^* &= \frac{\pi f^*(m_\Delta^*)}{4m_\Delta^*} \frac{|\mathcal{M}_{\pi N \rightarrow \Delta}^*|^2}{|\mathbf{k}|(E_N^* + \omega)} \\ &= \frac{2\pi^2 f^*(\sqrt{s}) \Gamma^*}{\mathbf{k}^2} \quad (18)\end{aligned}$$

with the effective mass take into account in the $|\mathcal{M}_{\pi N \rightarrow \Delta}^*|^2$ and mass distribution $f^*(m_\Delta^*) = f^*(\sqrt{s})$, i.e.,

$$f^* = \frac{2}{\pi} \frac{m_{0,\Delta}^{*2} \Gamma_t^*}{(m_{0,\Delta}^{*2} - m_\Delta^{*2})^2 + m_{0,\Delta}^{*2} \Gamma_t^{*2}}. \quad (19)$$

where Γ_t^* is the total decay width of $\Delta \rightarrow N\pi$ [46]. Here, the distributional Δ mass m_Δ^* in Eq. 15, 18 and 19 is the energy of $N\pi$ system in medium and is calculated based on the energy conservation relationship in Eq. (14), at given \mathbf{k} which corresponds to the center-of-mass of energy as $\sqrt{s} = m_\Delta = \sqrt{m_\pi^2 + \mathbf{k}^2} + \sqrt{m_N^2 + \mathbf{k}^2}$ in Δ static frame for free space, i.e., $m_\Delta^* \equiv m_\Delta^*(\sqrt{s})$. The Δ effective pole mass $m_{0,\Delta}^{*2}$ above is from Eq. 13. While, in Ref. [36], the effective mass on the spectral function of Δ resonance was not mentioned in the calculation of the cross sections of $N\pi \rightarrow \Delta$.

The coupling constants we used are determined by fitting the cross section of $\pi^+ + p \rightarrow \Delta^{++}$ and decay width in the free space [47]. The decay width of $\Delta \rightarrow N\pi$ in free space is:

$$\begin{aligned}\Gamma &= \frac{1}{2m_\Delta} \int \frac{d^3\mathbf{p}_N}{(2\pi)^3 2E_N} \frac{d^3\mathbf{p}_\pi}{(2\pi)^3 2\omega} \overline{|\mathcal{M}_{\Delta \rightarrow N\pi}|^2} \\ &\quad \times (2\pi)^4 \delta^3(\mathbf{p}_N + \mathbf{p}_\pi) \delta(E_N + \omega - m_\Delta) \\ &= \frac{\mathbf{k}^2}{8\pi m_\Delta E_N \omega} \frac{\overline{|\mathcal{M}_{\Delta \rightarrow N\pi}|^2}}{|\frac{\mathbf{k}}{E_N} + \frac{\mathbf{k}}{\omega}|} \quad (20)\end{aligned}$$

where $\mathbf{p}_\pi = \mathbf{k}$. Here $\overline{|\mathcal{M}_{\Delta \rightarrow N\pi}|^2}$ is calculated by:

$$\begin{aligned}\overline{|\mathcal{M}_{\Delta \rightarrow N\pi}|^2} &= \frac{1}{4} \sum_{s_\Delta} |\mathcal{M}_{\Delta \rightarrow N\pi}|^2 \\ &= \frac{g_{\pi N \Delta}^2 I_{N\Delta}^2}{4m_\pi^2} \sum_s \Psi(p_N) \bar{\Psi}(p_N) k^\mu \Delta_\mu(p_\Delta) \bar{\Delta}_\nu(p_\Delta) k^\nu \\ &= \frac{g_{\pi N \Delta}^2 I_{N\Delta}^2}{4m_\pi^2} \text{Tr}[(p_N + m_N) k^\mu \mathcal{P}_{\mu\nu}(p_\Delta) k^\nu] \\ &= \frac{2g_{\pi N \Delta}^2 I_{N\Delta}^2}{3m_\pi^2} (m_N + E_N) \mathbf{k}^2 m_\Delta \quad (21)\end{aligned}$$

The expression of the $\pi N \rightarrow \Delta$ cross section is

$$\begin{aligned}\sigma_{\pi N \rightarrow \Delta} &= \int dm_\Delta f(m_\Delta) \int \frac{d^3\mathbf{p}_\Delta}{(2\pi)^3 2E_\Delta} \frac{\overline{|\mathcal{M}_{\pi N \rightarrow \Delta}|^2}}{4E_N \omega |\frac{\mathbf{p}_N}{E_N} - \frac{\mathbf{k}}{\omega}|} \\ &\quad \times (2\pi)^4 \delta^3(\mathbf{p}_N + \mathbf{k} - \mathbf{p}_\Delta) \delta(E_N + \omega - E_\Delta). \quad (22)\end{aligned}$$

In the Δ static frame, $\sigma_{\pi N \rightarrow \Delta}$ can be written as

$$\sigma_{\pi N \rightarrow \Delta} = \frac{\pi f(m_\Delta)}{4m_\Delta E_N \omega} \frac{|\mathcal{M}_{\pi N \rightarrow \Delta}|^2}{|\frac{\mathbf{k}}{E_N} + \frac{\mathbf{k}}{\omega}|}. \quad (23)$$

where $|\mathcal{M}_{\pi N \rightarrow \Delta}|^2 = 2|\mathcal{M}_{\Delta \rightarrow N\pi}|^2$. The $f(m_\Delta)$ is the mass distribution of Δ resonance in free space, which reads

$$f(m_\Delta) = \frac{2}{\pi} \frac{m_{0,\Delta}^2 \Gamma_t}{(m_{0,\Delta}^2 - m_\Delta^2)^2 + m_{0,\Delta}^2 \Gamma_t^2}. \quad (24)$$

The coupling constants we used in Eq. 20, i.e., $g_{\pi NN} = 1.008$, $g_{\pi N\Delta} = 2.3$, and the cut-off $\Lambda^2 = \exp(-2\mathbf{k}^2/b^2)$ with $b = 7m_\pi$, which are fitted from the experimental data of cross section and decay width [47] in the Fig. 1. The decay width $\Gamma = 0.120$ GeV for the pole mass $m_\Delta = 1.232$ GeV can be calculated from Eq. 20.

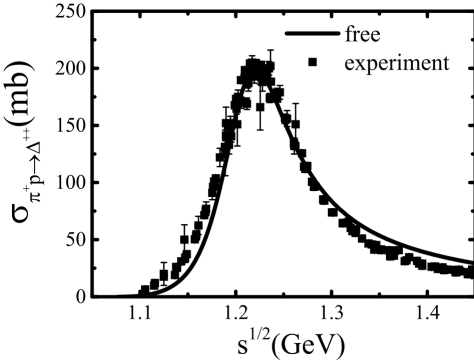


FIG. 1: (Color online) $\sigma_{\pi+p \rightarrow \Delta^{++}}$ as a function of $s^{1/2}$ in free space, the experimental data from Ref. [47].

III. RESULTS AND DISCUSSIONS

A. Pion dispersion relation

The pion dispersion relation has two solutions in Eq. (3), the lower one near the free pion energy $\omega_F = \sqrt{m_\pi^2 + k^2}$ named the particle-hole branch and higher one near the free $\omega_\Delta = \frac{k^2}{2m_\Delta} + m_\Delta - m_N$ named Δ -hole branch[31, 36]. Ref. [36] pointed out that the threshold for Δ resonance to decay into a pion in the Δ -hole branch is larger than 1.36 GeV. It makes the Δ decay into pion in Δ -hole branch is less important, if we focused on the effects near the Δ threshold energy. Thus, we neglect the decay of Δ into a pion in Δ -hole branch as in Ref. [36].

In the Fig. 2, we present the pion dispersion relation $\omega(k)$ and optical potential $V_\pi(k)$ at different densities in symmetric nuclear matter. The black solid, the red dashed, green dotted, blue dash-dotted and magenta dash-dotted lines represent the ω in free space, $0.5\rho_0$, ρ_0 ,

$1.5\rho_0$ and $2\rho_0$ respectively. The pion optical potential can be written as:

$$V_{\pi^i} = \omega_{\pi^i}(\mathbf{k}) - \sqrt{m_{\pi^i}^2 + \mathbf{k}^2}. \quad (25)$$

It can be seen from Fig. 2 that both the in-medium pion energy ω and the pion optical potential V_π do not vanish at $|\mathbf{k}| = 0$. It is because k^2 and $(pk)^2 - m_N^2 k^2$ appear in the relativistic form of Π_N and Π_Δ (see appendix B). The in-medium pion self energy do not vanish at momentum $|\mathbf{k}| = 0$, i.e. the color lines deviate the black line at $k=0$, which is different from the results in the nonrelativistic form of pion self-energy as in Ref. [36]. The in-medium pion energy ω increases with the density increasing at lower momentum ($|\mathbf{k}|/m_\pi < 0.6$) while decrease as density at higher momentum ($|\mathbf{k}|/m_\pi > 0.6$), where the results are the same as Refs. [31, 34]. In the right panel of Fig. 2, we present the pion optical potential for symmetric nuclear matter. The calculations results show that the pions with $|k|/m_\pi < 0.6$ feel a repulsive force, while the pions with $|k|/m_\pi > 0.6$ feel an attractive force. Consequently, one can expect that the pion spectral obtained in the heavy ion collisions may show their maximum values at certain kinetic energy comparing to the calculations without considering such pion potential. The energy slope of pion spectral may be a probe to investigate the pion optical potential. For the convenient applying the in-medium pion energy in estimation Δ decay width and optical potential in transport models, we give the parameterization form of ω as function of $|\mathbf{k}|$ in appendix D.

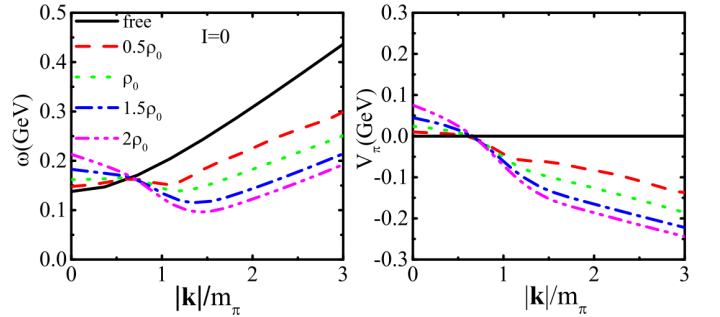


FIG. 2: (Color online) Left panel: the pion dispersion relation at different densities ($0.5\rho_0$, ρ_0 , $1.5\rho_0$ and $2\rho_0$) in symmetric nuclear matter. Right panel: the pion optical potential at different densities in symmetric nuclear matter.

In Fig. 3, we present the pion dispersion relation in asymmetric nuclear matter for $I = 0.2$, where $I = \frac{\rho_n - \rho_p}{\rho_n + \rho_p}$ is the isospin asymmetry. As shown in Fig. 3, the ω is split for different charge state of pions and the difference between $\omega(\pi^-)$ and $\omega(\pi^+)$ is related to the difference between the densities of neutron and proton, $\rho_n - \rho_p$, in asymmetric nuclear matter. Interestingly, one can say that $\omega(\pi^-) > \omega(\pi^+)$ at the $k < 0.6m_\pi$ and it turns over at $k > 0.6m_\pi$. This behaviors agree with the prediction from nonrelativistic calculation in Ref. [36] where

s-wave plus p-wave potential are adopted. While, the magnitude of the splitting of in-medium energy ω , i.e. $|\omega^- - \omega^+|$, evolving with density shows the different behaviors at $k < 0.6m_\pi$ and $k > 0.6m_\pi$. At $k < 0.6m_\pi$, $|\omega^- - \omega^+|$ monotonously increases with the nuclear density. At $k > 0.6m_\pi$, it firstly increases with density but starts to decrease with density above $1.5\rho_0$. The

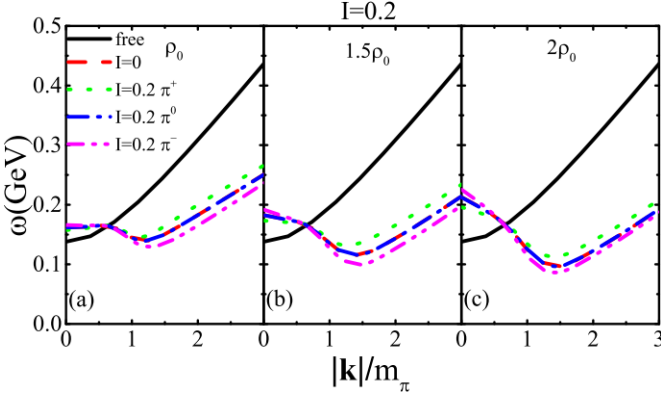


FIG. 3: (Color online) The pion dispersion relation at different densities (ρ_0 , $1.5\rho_0$ and $2\rho_0$) in asymmetric nuclear matter $I = 0.2$.

nonmonotonicity of $|\omega_{\pi^-} - \omega_{\pi^+}|$ with density increasing at $|\mathbf{k}|/m_\pi > 0.6$ can be more clearly seen in the difference of optical potential between π^- and π^+ , i.e. $\delta V_\pi = V_{\pi^-} - V_{\pi^+}$, in Fig. 4. The figures explicitly depict that δV_π approximatively reaches the maximum at $1.5\rho_0$ at higher momentum, where the isospin splitting effect is more obvious. In conclusion, the $\delta V_\pi = V_{\pi^-} - V_{\pi^+}$ is nonmonotonic in the relativistic calculations, which did not appear in the nonrelativistic one [36]. It could cause the enhancement of π^-/π^+ ratios at lower energy region, and the measurement of the energy spectral of π^-/π^+ in heavy ion collisions could be useful for deeply learning the in-medium energy of pion.

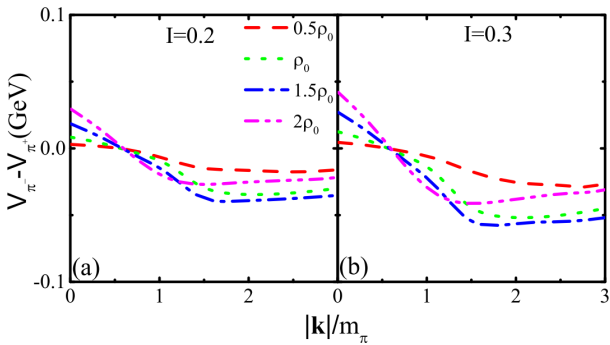


FIG. 4: (Color online) The left and right panel are $V_{\pi^-} - V_{\pi^+}$ at different densities in asymmetric nuclear matter at $I = 0.2$ and $I = 0.3$ respectively.

B. In-medium $\pi N \rightarrow \Delta$ cross sections and $\Delta \rightarrow \pi N$ decay widths

The energy conservation is an important issue that one should carefully handle in the calculation of $N\pi \rightarrow \Delta$ and $\Delta \rightarrow N\pi$ in isospin asymmetric nuclear matter as well as for $NN \rightarrow N\Delta$ [37], based on the formulas of the in-medium $\Delta \rightarrow N\pi$ decay widths and $N\pi \rightarrow \Delta$ cross sections, i.e., in Eq. (15) and (18). The Δ pole mass $m_{0,\Delta}^*$ and distribution function f^* are the crucial variable and key part besides $|\mathcal{M}_{\pi N \rightarrow \Delta}^*|^2$, because the $m_{0,\Delta}^*$ can determine the height and the position (\sqrt{s}) of the peak of f^* . Thus, we firstly analyze the values of $m_{0,\Delta}^*$ in the condition of energy conservation as Eq. (14).

The peak of f^* should be around the $m_{0,\Delta}^*$, which correspond to a certain momentum $|\mathbf{k}|_0$, or energy $s_0^{1/2}$, and it can satisfy the following relationship,

$$m_{0,\Delta}^* + \Sigma_\Delta^0 = \sqrt{m_N^* + |\mathbf{k}|_0^2 + \Sigma_N^0 + \omega(|\mathbf{k}|_0)}. \quad (26)$$

As shown in Fig. 2, $\omega(\mathbf{k})$ at normal density is reduced by 100-300 MeV as that in free space at $|\mathbf{k}|/m_\pi > 1.5$. Both $m_{0,\Delta}^*$ and m_N^* decrease with the density increasing, and $m_{0,\Delta}^* - m_N^* = m_{0,\Delta} - m_N$ with $|\Sigma_\Delta^0 - \Sigma_N^0| = 0$ in symmetric nuclear matter. In isospin asymmetric nuclear matter with $I = 0.2$, $m_{0,\Delta}^* - m_N^*$ and $|\Sigma_\Delta^0 - \Sigma_N^0|$ are about 40–50 MeV near $2\rho_0$. It indicates that the values of ω are the key quantities for determining the solution of $|\mathbf{k}|_0$ from Eq. 26. When the reductions of ω is taken into account and the energy conservation relationship is considered, a larger $|\mathbf{k}|_0$ is expected. Consequently, the position of the peak of f^* moves to the higher energy with smaller effective mass. In the left panel of Fig. 5, we present the $s_0^{1/2}$ as a function of $m_{0,\Delta}^*$. It clearly illustrates that the behaviors of $s_0^{1/2}$ increase with the effective mass decreasing, or equivalently with the increasing of the density. In the right panel of Fig. 5, the f^* as function of $s_0^{1/2}$ at different densities are presented in symmetric nuclear matter. Our results show that the f^* decreases with effective masses of nucleon and Δ , and the peak of f^* shifts to the higher momentum, which results in the reduction of in-medium $\pi N \rightarrow \Delta$ cross sections.

Based on the in-medium pion energy and effective masses of N and Δ , the in-medium cross section of $\pi^+ p \rightarrow \Delta^{++}$ and $\Delta \rightarrow \pi N$ decay width at different densities in symmetric nuclear matter are calculated based on Eq. (15) and (18), and they are presented in Fig. 6. As shown in the left panel, the in-medium $\Delta \rightarrow \pi N$ decay widths are enhanced relative to that in free space, but the effect is weak at the energy region we studied, because the impact of $m_\Delta^*(E_N^* + \omega)$ and $|\mathcal{M}_{\pi N \rightarrow \Delta}^*|^2$ in Eq. (20) conceal each other.

For the in-medium pion adsorption cross sections $\pi N \rightarrow \Delta$, as shown in the right panel of Fig. 6, they are suppressed at lower energy ($s^{1/2} < 1.25$ GeV) and enhanced at higher energy ($s^{1/2} > 1.25$ GeV). It can be understood from the effect of effective masses of N

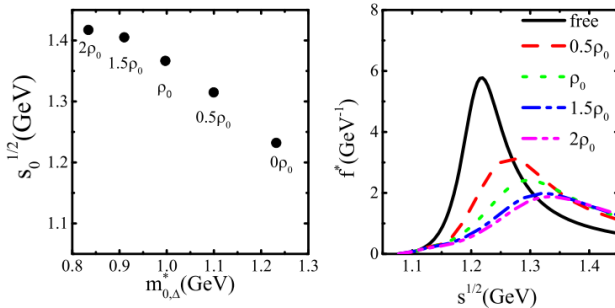


FIG. 5: (Color online) Left panel: the $s_0^{1/2}$ corresponding to the pion momentum $|\mathbf{k}|_0$ derived from the pole mass of Δ equation in Eq. 14. Right panel: f^* as function of $s^{1/2}$.

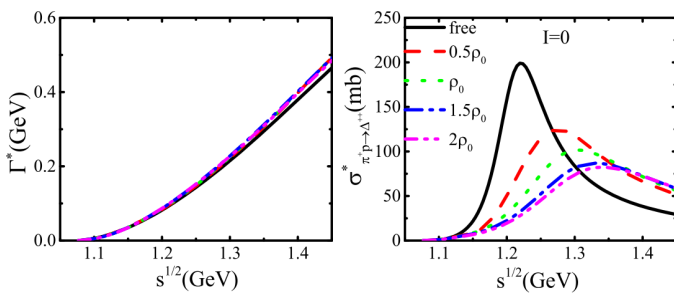


FIG. 6: (Color online) Left panel: in-medium decay width of $\Delta \rightarrow \pi N$ at different densities in symmetric nuclear matter. Right panel: in-medium cross sections of $\pi^+ p \rightarrow \Delta^{++}$ at different densities in symmetric nuclear matter.

and Δ on f^* . It could lead to the enhancement of pions in the HIC simulations near the threshold energy, since the smaller $\pi N \rightarrow \Delta$ cross sections weaken the second process of the loop of $\Delta - N - \pi$, i.e., process of $N\pi \rightarrow \Delta$, which make more π s are left to freeze out from the pion production process of $\Delta \rightarrow N\pi$. Our predictions on the in-medium effects on the $\pi N \rightarrow \Delta$ cross sections are different from the conclusion in Ref. [36], where they show the enhancement of in-medium $N\pi \rightarrow \Delta$ cross sections near the threshold energies. The different conclusions could come from the effects of effective masses on the Δ mass distributions which was not considered in Ref. [36], and it hints that a further experimental study of the pion production in heavy ion collisions will be useful for figuring out the in-medium $N\pi \rightarrow \Delta$.

Since the nuclear medium correction on the decay width of $\Delta \rightarrow \pi N$ is weak, we will focus on the in-medium cross sections of $N\pi \rightarrow \Delta$ in isospin asymmetric nuclear matter in the following discussions. In Fig. 7, we present the in-medium cross sections for $\pi^+ p \rightarrow \Delta^{++}$, $\pi^- n \rightarrow \Delta^-$, $\pi^0 p \rightarrow \Delta^+$, $\pi^0 n \rightarrow \Delta^0$, $\pi^+ n \rightarrow \Delta^+$ and $\pi^- p \rightarrow \Delta^0$ channels, respectively, in isospin asymmetric nuclear matter at densities of ρ_0 , $1.5\rho_0$ and $2\rho_0$ in asymmetric nuclear matter $I = 0.2$. If we do not consider the effective masses splitting, the ratios between the cross

sections of different channels are $\sigma_{\pi^+ p \rightarrow \Delta^{++}} / (\sigma_{\pi^- n \rightarrow \Delta^-})$: $\sigma_{\pi^0 p \rightarrow \Delta^+} / (\sigma_{\pi^- p \rightarrow \Delta^0})$: $\sigma_{\pi^+ n \rightarrow \Delta^+} / (\sigma_{\pi^- p \rightarrow \Delta^0}) = 3 : 2 : 1$, and the medium correction factors, i.e. $R = \sigma^* / \sigma^{\text{free}}$, are the same for different channels. With the nucleon and Δ effective masses splitting as well as pion energies in asymmetric nuclear matter to be considered, the in-medium correction factors R on the cross sections of $\pi N \rightarrow \Delta$ and $\Delta \rightarrow \pi N$ are different for different channels as the $\omega_{\pi^+} > \omega_{\pi^-}$ at higher energy and $m_{\Delta^{++}}^* > m_{\Delta^+}^* > m_{\Delta^0}^* > m_{\Delta^-}^*$, $m_p^* > m_n^*$. The $N\pi \rightarrow \Delta$ cross sections in asymmetric nuclear matter has the following sequence, i.e., $\sigma_{\pi^+ p \rightarrow \Delta^{++}}^* > \sigma_{\pi^- n \rightarrow \Delta^-}^*$, $\sigma_{\pi^0 p \rightarrow \Delta^+}^* > \sigma_{\pi^0 n \rightarrow \Delta^0}^*$, and $\sigma_{\pi^+ n \rightarrow \Delta^+}^* > \sigma_{\pi^- p \rightarrow \Delta^0}^*$ as in Fig. 7. Especially, the channels of $\pi^+ p \rightarrow \Delta^{++}$ and $\pi^- n \rightarrow \Delta^-$ clearly reveal this splitting effect.

The cross sections of $\pi^0 p \rightarrow \Delta^+$ and $\pi^0 n \rightarrow \Delta^0$ channels are in the middle panels (d)-(f) of Fig. 7, while in-medium cross sections of $\pi^+ n \rightarrow \Delta^+$ and $\pi^- p \rightarrow \Delta^0$ are presented in the bottom panel (g)-(i), both the cross sections and the splitting magnitude are smaller than those of the $\pi^+ p \rightarrow \Delta^{++}$ and $\pi^- n \rightarrow \Delta^-$ channels. Since the in-medium cross sections are reduced with density increasing, the splitting of the cross sections is also decreased, so the difference between the cross sections of channels $\pi^+ p \rightarrow \Delta^{++}$ and $\pi^- n \rightarrow \Delta^-$ at $1.5\rho_0$ is slightly smaller than that at ρ_0 .

The results are similar with work from Li, el at in Ref. [35], but the magnitude of the in-medium cross section and the splitting among the different channels are more obvious than that in Ref. [35], where the effect of ω in asymmetric nuclear matter is ignored. Based on above discussions on the in-medium cross section of $N\pi \rightarrow \Delta$, one can expect if one take $\sigma_{N\pi \rightarrow \Delta}^*$ in transport model simulations, the production of π^- will be enhanced relative to the utility of $\sigma_{N\pi \rightarrow \Delta}^{\text{free}}$.

IV. SUMMARY AND OUTLOOK

In summary, we have investigated the pion dispersion relation, in-medium $N\pi \rightarrow \Delta$ cross section and $\Delta \rightarrow N\pi$ decay width in isospin asymmetric nuclear matter by using the same relativistic interaction within the framework of one-boson-exchange model. With the consideration of threshold effect (or energy conservation in isospin asymmetric nuclear medium) and in-medium pion energy effect, the Δ mass distribution are suppressed and the position of peak of Δ mass distribution move to the high energy part with the density increasing (or effective mass decreasing). It results in a suppression of in-medium $N\pi \rightarrow \Delta$ cross sections near the low energy ($s^{1/2} < 1.25$ GeV) and enhancement in the high energy region ($s^{1/2} > 1.25$ GeV), which are different from the conclusion in Refs. [31, 36]. For the in-medium decay width of $\Delta \rightarrow N\pi$, it is enhanced by < 5%. Thus, the smaller $\pi N \rightarrow \Delta$ cross sections weaken the process of $N\pi \rightarrow \Delta$, and make more π s are left to freeze out during the pion production process of $\Delta \rightarrow N\pi$ in HICs.

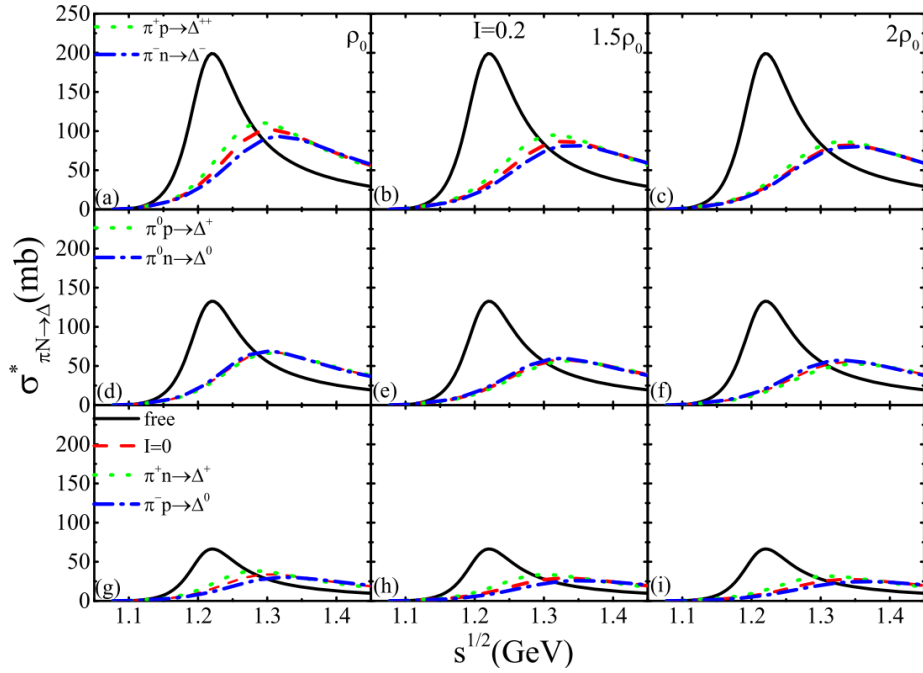


FIG. 7: (Color online) The in-medium cross sections of $\pi N \rightarrow \Delta$ for different channels at different densities (ρ_0 , $1.5\rho_0$ and $2\rho_0$) in asymmetric nuclear matter $I = 0.2$. Upper panel: $\pi^+ p \rightarrow \Delta^{++}$ and $\pi^- n \rightarrow \Delta^-$ channels. Middle panel: $\pi^0 p \rightarrow \Delta^+$ and $\pi^0 n \rightarrow \Delta^0$ channels. Bottom panel: $\pi^+ n \rightarrow \Delta^+$ and $\pi^- p \rightarrow \Delta^0$ channels.

By including the ω and effective mass splitting in asymmetric nuclear matter in the calculation of $N\pi \rightarrow \Delta$, our results show that the in-medium correction factors on the cross sections of $\pi N \rightarrow \Delta$ are different for different channels, i.e., $R_{\pi^+ p \rightarrow \Delta^{++}} > R_{\pi^- n \rightarrow \Delta^-}$. Applying the $\sigma_{N\pi \rightarrow \Delta}^*$ in transport model simulations especially near the threshold energy, it could predict a enhanced the total pion multiplicity and enhanced π^- multiplicity relative to the calculations utility of $\sigma_{N\pi \rightarrow \Delta}^{\text{free}}$, which hints a larger π^-/π^+ ratios could be observed near the threshold energy if the other parameters in transport model remain unchanged.

However, we should keep in mind that the simulation of heavy ion collision is much more complicated, our results suggest that a systematic study of pion production mechanism, from pion's multiplicity, energy spectral and flow, are needed. The beam energy scan, for example from subthreshold energy to 1.5 GeV/u, and system size dependence, from smaller systems to heavier systems, could be help us figure the medium effects on the cross sections of $N\pi \rightarrow \Delta$.

Acknowledgments

This work has been supported by National Key R&D Program of China under Grant No. 2018 YFA0404404, and National Natural Science Foundation of China under Grants No. 11875323, No. 11875125, No. 11475262, No. 11365004, No. 11375062, No. 11790323, 11790324, No.

11790325, and the Continuous Basic Scientific Research Project (No. WDJC-2019-13).

A. APPENDIX A

TABLE I: The isospin factors I_{NN} .

$NN\pi$	I_{NN}
$pp\pi^0$	1
$nn\pi^0$	-1
$pn\pi^+$	$-\sqrt{2}$
$np\pi^-$	$\sqrt{2}$

TABLE II: The isospin factors $I_{N\Delta}$.

Channel	$I_{N\Delta}$
$\Delta^{++} \rightarrow \pi^+ p$	1
$\Delta^+ \rightarrow \pi^+ n$	$\sqrt{\frac{1}{3}}$
$\Delta^+ \rightarrow \pi^0 p$	$\sqrt{\frac{2}{3}}$
$\Delta^0 \rightarrow \pi^0 n$	$\sqrt{\frac{2}{3}}$
$\Delta^0 \rightarrow \pi^- p$	$\sqrt{\frac{1}{3}}$
$\Delta^- \rightarrow \pi^- n$	1

B. APPENDIX B

For the on-shell pion dispersion relation in Eq. 3, the $\Pi(k)$ should be the real part ($\text{Re}\Pi(k)$), here all the $\Pi(k)$ are ignored the Re notion in the following. The particle-

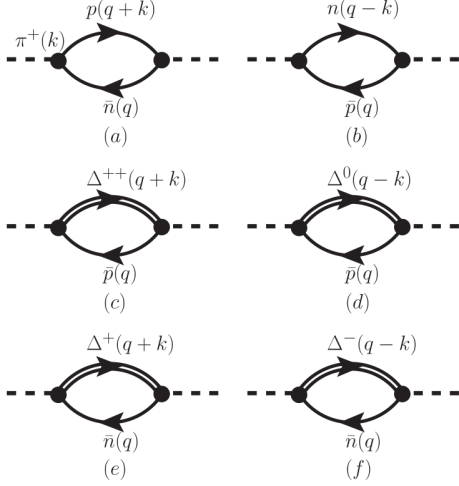


FIG. 8: The self-energy of $\pi^+(\omega, \mathbf{k})$, (a) and (b) are the particle-hole part, (c), (d), (e), (f) are the Δ -hole part.

hole part of the π^+ self-energy can be written as:

$$\Pi_N(\pi^+) = \Pi_a(\pi^+) + \Pi_b(\pi^+) \quad (27)$$

where $\Pi_a(\pi^+)$ is

$$\begin{aligned} \Pi_a(\pi^+) &= -i\left(\frac{\sqrt{2}g_{\pi NN}}{m_\pi}\right)^2 \int \frac{d^4q}{(2\pi)^4} \text{Tr} \left[\not{k}\gamma_5 \frac{\not{q} + m_n}{2E_n(q)} \not{k}\gamma_5 \right. \\ &\quad \times \frac{\not{q} + \not{k} + m_p}{(q_0 + k_0)^2 - E_p^2(q+k)} i2\pi\theta(q_{F,n} - |\mathbf{q}|) \delta(q^0 - E_n(q)) \left. \right] \\ &= \left(\frac{g_{\pi NN}}{m_\pi}\right)^2 \int \frac{d^4q}{(2\pi)^3} \theta(q_{F,n} - |\mathbf{q}|) \delta(q^0 - E_n(q)) \\ &\quad \times \frac{-4m_n m_p k^2 - 4q^2 k^2 + 8(qk)^2 + 4k^2(qk)}{E_n(q)((q_0 + k_0)^2 - E_p^2(q+k))} \\ &= \left(\frac{g_{\pi NN}}{m_\pi}\right)^2 \int \frac{d^3\mathbf{q}}{(2\pi)^3} \frac{\theta(q_{F,n} - |\mathbf{q}|)}{E_n(q)[(E_n(q) + \omega)^2 - E_p^2(q+k)]} \\ &\quad \times [-4m_n m_p k^2 - 4m_n^2 k^2 \\ &\quad + 4(E_n(q)\omega - \mathbf{q} \cdot \mathbf{k})(2E_n(q)\omega - \mathbf{q} \cdot \mathbf{k} + k^2)]. \end{aligned} \quad (28)$$

Here $k_0 = \omega$, $E_n(q) = \sqrt{m_n^2 + q^2}$ and $k^2 = k_0^2 - \mathbf{k}^2 = \omega^2 - \mathbf{k}^2$. And the isospin factor $I_{N\Delta} = -\sqrt{2}$ is listed in Table I. $\Pi_b(\pi^+)$ can also be calculated in the same way:

$$\begin{aligned} \Pi_b(\pi^+) &= -i\left(\frac{\sqrt{2}g_{\pi NN}}{m_\pi}\right)^2 \int \frac{d^4q}{(2\pi)^4} \text{Tr} \left[\not{k}\gamma_5 \frac{\not{q} + m_p}{2E_p(q)} \not{k}\gamma_5 \right. \\ &\quad \times \left. i2\pi\theta(q_{F,p} - |\mathbf{q}|) \delta(q^0 - E_p(q)) \right] \end{aligned}$$

$$\begin{aligned} &\times \not{k}\gamma_5 \frac{\not{q} - \not{k} + m_n}{(q_0 - k_0)^2 - E_n^2(q-k)} \\ &\times i2\pi\theta(q_{F,p} - |\mathbf{q}|) \delta(q^0 - E_p(q)) \end{aligned} \quad (29)$$

$$\begin{aligned} &= \left(\frac{g_{\pi NN}}{m_\pi}\right)^2 \int \frac{d^3\mathbf{q}}{(2\pi)^3} \frac{\theta(q_{F,p} - |\mathbf{q}|)}{E_p(q)[(E_p(q) - \omega)^2 - E_n^2(q-k)]} \\ &\quad \times [-4m_n m_p k^2 - 4m_p^2 k^2 \\ &\quad + 4(-E_p(q)\omega + \mathbf{q} \cdot \mathbf{k})(-2E_p(q)\omega + \mathbf{q} \cdot \mathbf{k} + k^2)]. \end{aligned} \quad (30)$$

The Δ -hole part of the π^+ self-energy is:

$$\Pi_\Delta(\pi^+) = \Pi_c(\pi^+) + \Pi_d(\pi^+) + \Pi_e(\pi^+) + \Pi_f(\pi^+) \quad (31)$$

where $\Pi_c(\pi^+)$

$$\begin{aligned} \Pi_c(\pi^+) &= -i\left(\frac{g_{\pi N\Delta}}{m_\pi}\right)^2 \int \frac{d^4q}{(2\pi)^4} \text{Tr} \left[\frac{k_\mu k_\nu D^{\mu\nu}(q+k)(\not{q} + \not{k} + m_{0,\Delta})}{(q_0 + k_0)^2 - E_\Delta^2(q+k)} \right. \\ &\quad \times \frac{\not{q} + m_n}{2E_p(q)} \theta(q_{F,p} - |\mathbf{q}|) (i2\pi\delta(q_0 - E_p(q))) \left. \right] \\ &= \left(\frac{g_{\pi N\Delta}}{m_\pi}\right)^2 \int \frac{d^3\mathbf{q}}{(2\pi)^3} \frac{\theta(q_{F,p} - |\mathbf{q}|)}{2E_p(q)((E_p(q) + k_0)^2 - E_\Delta^2(q+k))} \\ &\quad \times 4 \left[\frac{2m_p(qk)^2}{3m_{0,\Delta^{++}}} + \frac{4m_p(qk)k^2}{3m_{0,\Delta^{++}}} + \frac{2m_p k^4}{3m_{0,\Delta^{++}}} - \frac{2m_p m_{0,\Delta^{++}} k^2}{3} \right. \\ &\quad + \frac{2q^2 k^4}{3m_{0,\Delta^{++}}^2} + \frac{2(qk)^3}{3m_{0,\Delta^{++}}^2} + \frac{2q^2(qk)^2}{3m_{0,\Delta^{++}}^2} + \frac{4k^2(qk)^2}{3m_{0,\Delta^{++}}^2} \\ &\quad + \frac{2k^4(qk)}{3m_{0,\Delta^{++}}^2} + \frac{4q^2 k^2(qk)}{3m_{0,\Delta^{++}}^2} - \frac{2q^2 k^2}{3} - \frac{2k^2(pk)}{3} \left. \right] \\ &= \frac{2}{3} \left(\frac{g_{\pi N\Delta}}{m_\pi}\right)^2 \int \frac{d^3\mathbf{q}}{(2\pi)^3} \frac{\theta(q_{F,p} - |\mathbf{q}|)}{E_p(q)} \\ &\quad \times \left[\frac{(qk)^2 - m_p^2 k^2}{m_{0,\Delta^{++}}^2} + k^2 \frac{2m_p}{m_{0,\Delta^{++}}} \left(1 + \frac{m_p}{m_{0,\Delta^{++}}}\right) \right. \\ &\quad + \frac{(qk)^2 - m_p^2 k^2}{m_{0,\Delta^{++}}^2} \frac{(m_p + m_{0,\Delta^{++}})^2 - k^2}{2qk + k^2 - (m_{0,\Delta^{++}}^2 - m_p^2)} \left. \right], \end{aligned} \quad (32)$$

where $qk = E_p(q)\omega - \mathbf{q} \cdot \mathbf{k}$. $\Pi_d(\pi^+)$, $\Pi_e(\pi^+)$ and $\Pi_f(\pi^+)$ can be obtained in the same way:

$$\begin{aligned} \Pi_d(\pi^+) &= \frac{2}{9} \left(\frac{g_{\pi N\Delta}}{m_\pi}\right)^2 \int \frac{d^3\mathbf{q}}{(2\pi)^3} \frac{\theta(q_{F,p} - |\mathbf{q}|)}{E_p(q)} \\ &\quad \times \left[\frac{(qk)^2 - m_p^2 k^2}{m_{0,\Delta^0}^2} + k^2 \frac{2m_p}{m_{0,\Delta^0}} \left(1 + \frac{m_p}{m_{0,\Delta^0}}\right) \right. \\ &\quad + \frac{(qk)^2 - m_p^2 k^2}{m_{0,\Delta^0}^2} \frac{(m_p + m_{0,\Delta^0})^2 - k^2}{-2qk + k^2 - (m_{0,\Delta^0}^2 - m_p^2)} \left. \right], \end{aligned} \quad (33)$$

$$\Pi_e(\pi^+)$$

$$\begin{aligned}
&= \frac{2}{9} \left(\frac{g_{\pi N \Delta}}{m_\pi} \right)^2 \int \frac{d^3 \mathbf{q}}{(2\pi)^3} \frac{\theta(q_{F,n} - |\mathbf{q}|)}{E_n(q)} \\
&\times \left[\frac{(qk)^2 - m_n^2 k^2}{m_{0,\Delta^+}^2} + k^2 \frac{2m_n}{m_{0,\Delta^+}} \left(1 + \frac{m_n}{m_{0,\Delta^+}} \right) \right. \\
&\left. + \frac{(qk)^2 - m_n^2 k^2}{m_{0,\Delta^+}^2} \frac{(m_n + m_{0,\Delta^+})^2 - k^2}{2qk + k^2 - (m_{0,\Delta^+}^2 - m_n^2)} \right], \\
\end{aligned} \tag{34}$$

$$\begin{aligned}
\Pi_f(\pi^+) \\
&= \frac{2}{3} \left(\frac{g_{\pi N \Delta}}{m_\pi} \right)^2 \int \frac{d^3 \mathbf{q}}{(2\pi)^3} \frac{\theta(q_{F,n} - |\mathbf{q}|)}{E_n(q)} \\
&\times \left[\frac{(qk)^2 - m_n^2 k^2}{m_{0,\Delta^-}^2} + k^2 \frac{2m_n}{m_{0,\Delta^-}} \left(1 + \frac{m_n}{m_{0,\Delta^-}} \right) \right. \\
&\left. + \frac{(qk)^2 - m_n^2 k^2}{m_{0,\Delta^-}^2} \frac{(m_n + m_{0,\Delta^-})^2 - k^2}{-2qk + k^2 - (m_{0,\Delta^-}^2 - m_n^2)} \right]. \\
\end{aligned} \tag{35}$$

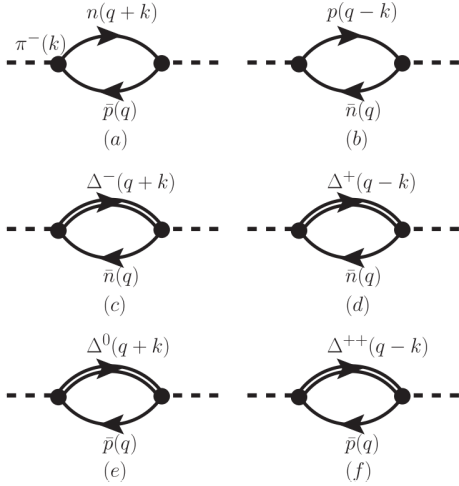


FIG. 9: $\pi^-(\omega, \mathbf{k})$ self-energy

The particle-hole part of the π^- self-energy can be written as:

$$\Pi_N(\pi^-) = \Pi_a(\pi^-) + \Pi_b(\pi^-) \tag{36}$$

Here $\Pi_a(\pi^-)$ and $\Pi_b(\pi^-)$ are in the following:

$$\begin{aligned}
\Pi_a(\pi^-) \\
&= \left(\frac{g_{\pi N N}}{m_\pi} \right)^2 \int \frac{d^3 \mathbf{q}}{(2\pi)^3} \frac{\theta(q_{F,p} - |\mathbf{q}|)}{E_p(q)[(E_p(q) + \omega)^2 - E_n^2(q + k)]} \\
&\times [-4m_n m_p k^2 - 4m_p^2 k^2 \\
&+ 4(E_p(q)\omega - \mathbf{q} \cdot \mathbf{k})(2E_p(q)\omega - \mathbf{q} \cdot \mathbf{k} + k^2)]. \\
\end{aligned} \tag{37}$$

$$\Pi_b(\pi^-)$$

$$\begin{aligned}
&= \left(\frac{g_{\pi N N}}{m_\pi} \right)^2 \int \frac{d^3 \mathbf{q}}{(2\pi)^3} \frac{\theta(q_{F,p} - |\mathbf{q}|)}{E_p(q)[(E_n(q) - \omega)^2 - E_p^2(q - k)]} \\
&\times [-4m_n m_p k^2 - 4m_n^2 k^2 \\
&+ 4(-E_n(q)\omega + \mathbf{q} \cdot \mathbf{k})(-2E_n(q)\omega + \mathbf{q} \cdot \mathbf{k} + k^2)]. \\
\end{aligned} \tag{38}$$

The Δ -hole part of the π^- self-energy is:

$$\Pi_\Delta(\pi^-) = \Pi_c(\pi^-) + \Pi_d(\pi^-) + \Pi_e(\pi^-) + \Pi_f(\pi^-) \tag{39}$$

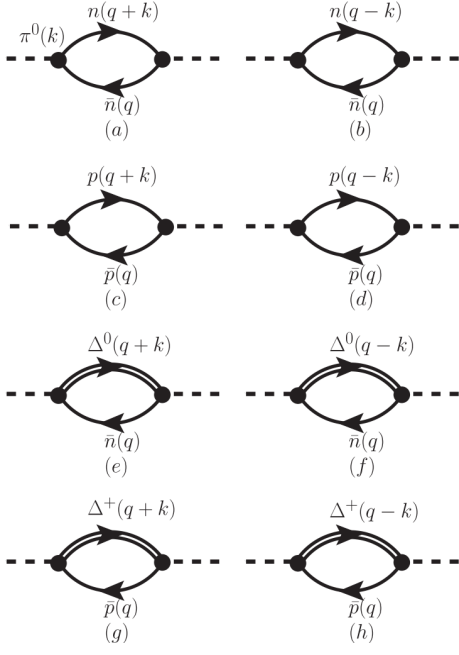
Here $\Pi_c(\pi^-)$, $\Pi_d(\pi^-)$, $\Pi_e(\pi^-)$ and $\Pi_f(\pi^-)$ can be calculated in the following:

$$\begin{aligned}
\Pi_c(\pi^-) \\
&= \frac{2}{3} \left(\frac{g_{\pi N \Delta}}{m_\pi} \right)^2 \int \frac{d^3 \mathbf{q}}{(2\pi)^3} \frac{\theta(q_{F,n} - |\mathbf{q}|)}{E_n(q)} \\
&\times \left[\frac{(qk)^2 - m_n^2 k^2}{m_{0,\Delta^+}^2} + k^2 \frac{2m_n}{m_{0,\Delta^+}} \left(1 + \frac{m_n}{m_{0,\Delta^+}} \right) \right. \\
&\left. + \frac{(qk)^2 - m_n^2 k^2}{m_{0,\Delta^+}^2} \frac{(m_n + m_{0,\Delta^+})^2 - k^2}{2qk + k^2 - (m_{0,\Delta^+}^2 - m_n^2)} \right], \\
\end{aligned} \tag{40}$$

$$\begin{aligned}
\Pi_d(\pi^-) \\
&= \frac{2}{9} \left(\frac{g_{\pi N \Delta}}{m_\pi} \right)^2 \int \frac{d^3 \mathbf{q}}{(2\pi)^3} \frac{\theta(q_{F,n} - |\mathbf{q}|)}{E_n(q)} \\
&\times \left[\frac{(qk)^2 - m_n^2 k^2}{m_{0,\Delta^-}^2} + k^2 \frac{2m_n}{m_{0,\Delta^-}} \left(1 + \frac{m_n}{m_{0,\Delta^-}} \right) \right. \\
&\left. + \frac{(qk)^2 - m_n^2 k^2}{m_{0,\Delta^-}^2} \frac{(m_n + m_{0,\Delta^-})^2 - k^2}{-2qk + k^2 - (m_{0,\Delta^-}^2 - m_n^2)} \right], \\
\end{aligned} \tag{41}$$

$$\begin{aligned}
\Pi_e(\pi^-) \\
&= \frac{2}{9} \left(\frac{g_{\pi N \Delta}}{m_\pi} \right)^2 \int \frac{d^3 \mathbf{q}}{(2\pi)^3} \frac{\theta(q_{F,p} - |\mathbf{q}|)}{E_p(q)} \\
&\times \left[\frac{(qk)^2 - m_p^2 k^2}{m_{0,\Delta^0}^2} + k^2 \frac{2m_p}{m_{0,\Delta^0}} \left(1 + \frac{m_p}{m_{0,\Delta^0}} \right) \right. \\
&\left. + \frac{(qk)^2 - m_p^2 k^2}{m_{0,\Delta^0}^2} \frac{(m_p + m_{0,\Delta^0})^2 - k^2}{2qk + k^2 - (m_{0,\Delta^0}^2 - m_p^2)} \right], \\
\end{aligned} \tag{42}$$

$$\begin{aligned}
\Pi_f(\pi^-) \\
&= \frac{2}{3} \left(\frac{g_{\pi N \Delta}}{m_\pi} \right)^2 \int \frac{d^3 \mathbf{q}}{(2\pi)^3} \frac{\theta(q_{F,p} - |\mathbf{q}|)}{E_p(q)} \\
&\times \left[\frac{(qk)^2 - m_p^2 k^2}{m_{0,\Delta^{++}}^2} + k^2 \frac{2m_p}{m_{0,\Delta^{++}}} \left(1 + \frac{m_p}{m_{0,\Delta^{++}}} \right) \right. \\
&\left. + \frac{(qk)^2 - m_p^2 k^2}{m_{0,\Delta^{++}}^2} \frac{(m_p + m_{0,\Delta^{++}})^2 - k^2}{-2qk + k^2 - (m_{0,\Delta^{++}}^2 - m_p^2)} \right]. \\
\end{aligned} \tag{43}$$

FIG. 10: $\pi^0(\omega, \mathbf{k})$ self-energy

The particle-hole part of the π^0 self-energy can be written as:

$$\Pi_N(\pi^0) = \Pi_a(\pi^0) + \Pi_b(\pi^0) + \Pi_c(\pi^0) + \Pi_d(\pi^0). \quad (44)$$

Here $\Pi_a(\pi^0)$, $\Pi_b(\pi^0)$, $\Pi_c(\pi^0)$ and $\Pi_d(\pi^0)$ are in the following:

$$\begin{aligned} \Pi_a(\pi^0) &= \left(\frac{g_{\pi NN}}{m_\pi}\right)^2 \int \frac{d^3 \mathbf{q}}{(2\pi)^3} \theta(q_{F,n} - |\mathbf{q}|) \\ &\times \left[\frac{-4m_n^2 k^2}{E_n(q)(2E_n(q)\omega - 2\mathbf{q} \cdot \mathbf{k} + \omega^2 - \mathbf{k}^2)} + 2\omega \right], \end{aligned} \quad (45)$$

$$\begin{aligned} \Pi_b(\pi^0) &= \left(\frac{g_{\pi NN}}{m_\pi}\right)^2 \int \frac{d^3 \mathbf{q}}{(2\pi)^3} \theta(q_{F,n} - |\mathbf{q}|) \\ &\times \left[\frac{-4m_n^2 k^2}{E_n(q)(-2E_n(q)\omega + 2\mathbf{q} \cdot \mathbf{k} + \omega^2 - \mathbf{k}^2)} - 2\omega \right], \end{aligned} \quad (46)$$

$$\begin{aligned} \Pi_c(\pi^0) &= \left(\frac{g_{\pi NN}}{m_\pi}\right)^2 \int \frac{d^3 \mathbf{q}}{(2\pi)^3} \theta(q_{F,p} - |\mathbf{q}|) \\ &\times \left[\frac{-4m_p^2 k^2}{E_p(q)(2E_p(q)\omega - 2\mathbf{q} \cdot \mathbf{k} + \omega^2 - \mathbf{k}^2)} + 2\omega \right], \end{aligned} \quad (47)$$

$$\begin{aligned} \Pi_d(\pi^0) &= \left(\frac{g_{\pi NN}}{m_\pi}\right)^2 \int \frac{d^3 \mathbf{q}}{(2\pi)^3} \theta(q_{F,p} - |\mathbf{q}|) \\ &\times \left[\frac{-4m_p^2 k^2}{E_p(q)(-2E_p(q)\omega + 2\mathbf{q} \cdot \mathbf{k} + \omega^2 - \mathbf{k}^2)} - 2\omega \right]. \end{aligned} \quad (48)$$

The Δ -hole part of the π^- self-energy is:

$$\Pi_\Delta(\pi^0) = \Pi_e(\pi^0) + \Pi_f(\pi^0) + \Pi_g(\pi^0) + \Pi_h(\pi^0). \quad (49)$$

Here $\Pi_e(\pi^0)$, $\Pi_f(\pi^0)$, $\Pi_g(\pi^0)$ and $\Pi_h(\pi^0)$ can be calculated in the following:

$$\begin{aligned} \Pi_e(\pi^0) &= \frac{4}{9} \left(\frac{g_{\pi N\Delta}}{m_\pi}\right)^2 \int \frac{d^3 \mathbf{q}}{(2\pi)^3} \frac{\theta(q_{F,n} - |\mathbf{q}|)}{E_n(q)} \\ &\times \left[\frac{(qk)^2 - m_n^2 k^2}{m_{0,\Delta^0}^2} + k^2 \frac{2m_n}{m_{0,\Delta^0}} \left(1 + \frac{m_n}{m_{0,\Delta^0}}\right) \right. \\ &\left. + \frac{(qk)^2 - m_n^2 k^2}{m_{0,\Delta^0}^2} \frac{(m_n + m_{0,\Delta^0})^2 - k^2}{2qk + k^2 - (m_{0,\Delta^0}^2 - m_n^2)} \right], \end{aligned} \quad (50)$$

$$\begin{aligned} \Pi_f(\pi^0) &= \frac{4}{9} \left(\frac{g_{\pi N\Delta}}{m_\pi}\right)^2 \int \frac{d^3 \mathbf{q}}{(2\pi)^3} \frac{\theta(q_{F,n} - |\mathbf{q}|)}{E_n(q)} \\ &\times \left[\frac{(qk)^2 - m_n^2 k^2}{m_{0,\Delta^0}^2} + k^2 \frac{2m_n}{m_{0,\Delta^0}} \left(1 + \frac{m_n}{m_{0,\Delta^0}}\right) \right. \\ &\left. + \frac{(qk)^2 - m_n^2 k^2}{m_{0,\Delta^0}^2} \frac{(m_n + m_{0,\Delta^0})^2 - k^2}{-2qk + k^2 - (m_{0,\Delta^0}^2 - m_n^2)} \right], \end{aligned} \quad (51)$$

$$\begin{aligned} \Pi_g(\pi^0) &= \frac{4}{9} \left(\frac{g_{\pi N\Delta}}{m_\pi}\right)^2 \int \frac{d^3 \mathbf{q}}{(2\pi)^3} \frac{\theta(q_{F,p} - |\mathbf{q}|)}{E_p(q)} \\ &\times \left[\frac{(qk)^2 - m_p^2 k^2}{m_{0,\Delta^+}^2} + k^2 \frac{2m_p}{m_{0,\Delta^+}} \left(1 + \frac{m_p}{m_{0,\Delta^+}}\right) \right. \\ &\left. + \frac{(qk)^2 - m_p^2 k^2}{m_{0,\Delta^+}^2} \frac{(m_p + m_{0,\Delta^+})^2 - k^2}{2qk + k^2 - (m_{0,\Delta^+}^2 - m_p^2)} \right], \end{aligned} \quad (52)$$

$$\begin{aligned} \Pi_h(\pi^0) &= \frac{4}{9} \left(\frac{g_{\pi N\Delta}}{m_\pi}\right)^2 \int \frac{d^3 \mathbf{q}}{(2\pi)^3} \frac{\theta(q_{F,p} - |\mathbf{q}|)}{E_p(q)} \\ &\times \left[\frac{(qk)^2 - m_p^2 k^2}{m_{0,\Delta^+}^2} + k^2 \frac{2m_p}{m_{0,\Delta^+}} \left(1 + \frac{m_p}{m_{0,\Delta^+}}\right) \right. \\ &\left. + \frac{(qk)^2 - m_p^2 k^2}{m_{0,\Delta^+}^2} \frac{(m_p + m_{0,\Delta^+})^2 - k^2}{-2qk + k^2 - (m_{0,\Delta^+}^2 - m_p^2)} \right]. \end{aligned} \quad (53)$$

In symmetric nuclear matter, the pion self energy is :

$$\begin{aligned} \Pi_N &= -8m_N^2 k^2 \left(\frac{g_{\pi NN}}{m_\pi} \right)^2 \int \frac{d^3 \mathbf{q}}{(2\pi)^3} \frac{\theta(q_{F,N} - |\mathbf{q}|)}{E_N(q)} \\ &\times \left[\frac{1}{2E_N(q)\omega - 2\mathbf{q} \cdot \mathbf{k} + \omega^2 - \mathbf{k}^2} \right. \\ &\left. - \frac{1}{-2E_N(q)\omega + 2\mathbf{q} \cdot \mathbf{k} + \omega^2 - \mathbf{k}^2} \right], \end{aligned} \quad (54)$$

and

$$\begin{aligned} \Pi_\Delta &= \frac{8}{9} \left(\frac{g_{\pi N\Delta}}{m_\pi} \right)^2 \int \frac{d^3 \mathbf{q}}{(2\pi)^3} \frac{\theta(q_{F,N} - |\mathbf{q}|)}{E_N(q)} \\ &\times \left\{ \frac{(qk)^2 - m_N^2 k^2}{m_{0,\Delta}^2} + k^2 \frac{2m_N}{m_{0,\Delta}} \left(1 + \frac{m_N}{m_{0,\Delta}} \right) \right. \\ &+ \frac{(qk)^2 - m_N^2 k^2}{m_{0,\Delta}^2} \left[\frac{(m_N + m_{0,\Delta})^2 - k^2}{2qk + k^2 - (m_{0,\Delta}^2 - m_N^2)} \right. \\ &\left. \left. + \frac{(m_N + m_{0,\Delta})^2 - k^2}{-2qk + k^2 - (m_{0,\Delta}^2 - m_N^2)} \right] \right\}. \end{aligned} \quad (55)$$

C. APPENDIX C

The pion self-energies in Appendix A can be expressed in terms of an analog of the susceptibility χ as follows

$$\Pi_N = k^2 \chi_N \quad (56)$$

$$\Pi_\Delta = k^2 \chi_\Delta. \quad (57)$$

Here we introduce the effect nonrelativistic interaction as the nuclear spin-isospin short range correlation as Ref.[34]:

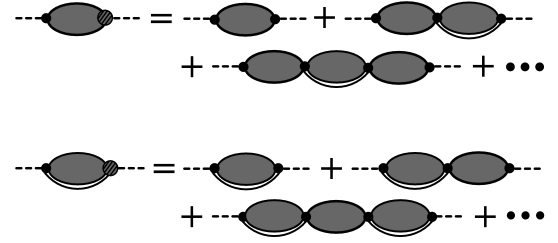
$$\begin{aligned} W &= \left(\frac{g_{\pi NN}}{m_\pi} \right)^2 g'_{NN} \boldsymbol{\sigma}_1 \cdot \boldsymbol{\sigma}_2 \boldsymbol{\tau}_1 \cdot \boldsymbol{\tau}_2 \\ &+ \left(\frac{g_{\pi N\Delta}}{m_\pi} \right)^2 g'_{\Delta\Delta} \boldsymbol{S}_1^\dagger \cdot \boldsymbol{S}_2 \boldsymbol{\tau}_1^\dagger \cdot \boldsymbol{\tau}_2 \\ &+ \frac{g_{\pi NN} g_{\pi N\Delta}}{m_\pi^2} g'_{N\Delta} \boldsymbol{S}_1^\dagger \cdot \boldsymbol{\sigma}_2 \boldsymbol{\tau}_1^\dagger \cdot \boldsymbol{\tau}_2 + h.c. \end{aligned} \quad (58)$$

With the short-range interaction, the pion dispersion relation can be:

$$\omega^2 = m_\pi^2 + \mathbf{k}^2 + \Pi = m_\pi^2 + \mathbf{k}^2 + k^2 \chi \quad (59)$$

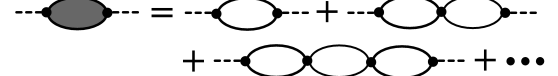


$$\chi = \chi_1 + \chi_2 \quad (60)$$



$$\chi_1 = \chi'_N \frac{1 + g'_{N\Delta} \chi'_\Delta}{1 - g'_{N\Delta} \chi'_\Delta g'_{N\Delta} \chi'_N} \quad (61)$$

$$\chi_2 = \chi'_\Delta \frac{1 + g'_{N\Delta} \chi'_N}{1 - g'_{N\Delta} \chi'_N g'_{N\Delta} \chi'_\Delta}. \quad (62)$$



$$\chi'_N = \frac{\chi_N}{1 - g'_{NN} \chi_N} \quad (63)$$

$$\chi'_\Delta = \frac{\chi_\Delta}{1 - g'_{\Delta\Delta} \chi_\Delta}. \quad (64)$$

Then the susceptibility can be written as:

$$\begin{aligned} \chi_N \rightarrow \chi_1 &= \frac{1 + (g'_{N\Delta} - g'_{\Delta\Delta}) \chi_\Delta}{(1 - g'_{\Delta\Delta} \chi_\Delta)(1 - g'_{NN} \chi_N) - g'_{N\Delta} \chi_\Delta g'_{N\Delta} \chi_N} \chi_N \\ \chi_\Delta \rightarrow \chi_2 &= \frac{1 + (g'_{N\Delta} - g'_{NN}) \chi_N}{(1 - g'_{\Delta\Delta} \chi_\Delta)(1 - g'_{NN} \chi_N) - g'_{N\Delta} \chi_\Delta g'_{N\Delta} \chi_N} \chi_\Delta \end{aligned} \quad (65)$$

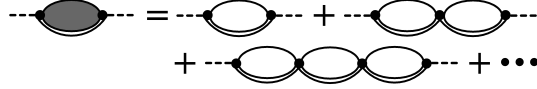
D. APPENDIX D

The pion energy ω in the nuclear matter can be written as the parametrization form

$$\omega = a_0 + a_1 x + a_2 x^2 + a_3 x^3 + a_4 x^4 + a_5 x^5 + a_6 x^6 \quad (66)$$

where $x = |\mathbf{k}|/m_\pi$, and $a_0, a_1, a_2, a_3, a_4, a_5, a_6$ are all in GeV.

Here parametrization form of $\omega(\pi^0)$ at $I = 0.3$ and $I = 0.2$ is the same as symmetric nuclear matter.

TABLE III: The parameters for ω in symmetric nuclear matter.

Density	x	a_0	a_1	a_2	a_3	a_4	a_5	a_6
$0.5\rho_0$	$x \leq 1.125$	0.14762	0.00329	0.15947	-1.09393	3.2301	-3.73303	1.42962
	$x > 1.125$	-0.08538	-0.99954	3.29955	-3.44383	1.71089	-0.41244	0.03884
ρ_0	$x \leq 1.125$	0.16428	-0.10651	0.5233	-0.72545	0.28734	0	0
	$x > 1.125$	0.40054	-0.63405	0.50715	-0.15842	0.0181	0	0
$1.5\rho_0$	$x \leq 1.125$	0.18147	0.04198	-0.53115	1.52268	-1.70649	0.62449	0
	$x > 1.125$	0.66757	-1.15148	0.83679	-0.25277	0.02837	0	0
$2\rho_0$	$x \leq 1.125$	0.21177	-0.0107	-0.35514	0.96565	-1.09207	0.40349	0
	$x > 1.125$	0.83163	-1.50549	1.08558	-0.3289	0.03692	0	0

TABLE IV: The parameters for ω_{π^+} at isospin asymmetry $I = 0.2$.

Density	x	a_0	a_1	a_2	a_3	a_4	a_5	a_6
$0.5\rho_0$	$x \leq 1.125$	0.14646	-0.01197	0.3134	-1.66811	4.26204	-4.60666	1.7103
	$x > 1.125$	-0.07165	0.26725	-0.0744	0.00899	0	0	0
ρ_0	$x \leq 1.125$	0.15305	0.14062	-1.03791	2.95229	-3.30208	1.23473	0
	$x > 1.125$	0.10479	-0.03411	0.08511	-0.02918	0.00353	0	0
$1.5\rho_0$	$x \leq 1.125$	0.16982	0.09594	-0.78495	2.17423	-2.39857	0.88103	0
	$x > 1.125$	0.36904	-0.54203	0.41088	-0.1227	0.01366	0	0
$2\rho_0$	$x \leq 1.125$	0.19358	0.04438	-0.57001	1.53095	-1.67771	0.61064	0
	$x > 1.125$	1.36471	-3.0588	2.86344	-1.30201	0.29304	-0.02607	0

TABLE V: The parameters for ω_{π^-} at isospin asymmetry $I = 0.2$.

Density	x	a_0	a_1	a_2	a_3	a_4	a_5	a_6
$0.5\rho_0$	$x \leq 1.125$	0.14953	-0.0217	0.40913	-2.12781	5.18789	-5.4529	1.99392
	$x > 1.125$	-0.03752	0.2044	-0.04916	0.00566	0	0	0
ρ_0	$x \leq 1.125$	0.16601	-0.01132	0.14963	-0.30154	0.13559	0	0
	$x > 1.125$	0.49951	-0.77281	0.55235	-0.15885	0.01696	0	0
$1.5\rho_0$	$x \leq 1.125$	0.18891	0.05333	-0.64292	1.713	-1.85345	0.6668	0
	$x > 1.125$	0.86713	-1.568	1.12794	-0.34088	0.03816	0	0
$2\rho_0$	$x \leq 1.125$	0.2235	-2.27582	-0.53085	1.3709	-1.51562	0.56282	0
	$x > 1.125$	1.65668	-3.85346	3.62636	-1.65695	0.37366	-0.03324	0

TABLE VI: The parameters for ω_{π^+} at isospin asymmetry $I = 0.3$.

Density	x	a_0	a_1	a_2	a_3	a_4	a_5	a_6
$0.5\rho_0$	$x \leq 1.125$	0.14561	-0.01313	0.33908	-1.79495	4.55558	-4.90908	1.822
	$x > 1.125$	-0.06849	0.25597	-0.06608	0.00771	0	0	0
ρ_0	$x \leq 1.125$	0.15103	0.13677	-1.00479	2.89048	-3.2475	1.2163	0
	$x > 1.125$	0.02613	0.11939	-0.01774	0.00182	0	0	0
$1.5\rho_0$	$x \leq 1.125$	0.19645	-0.07531	0.39858	-1.90247	4.05329	-3.87382	1.32371
	$x > 1.125$	1.9563	-4.52087	4.22417	-1.92159	0.4317	-0.03829	0
$2\rho_0$	$x \leq 1.125$	0.18406	0.07659	-0.71693	1.92654	-2.10031	0.76536	0
	$x > 1.125$	0.50864	-0.82079	0.60002	-0.17954	0.02003	0	0

TABLE VII: The parameters for ω_{π^-} at isospin asymmetry $I = 0.3$.

Density	x	a_0	a_1	a_2	a_3	a_4	a_5	a_6
$0.5\rho_0$	$x \leq 1.125$	0.14982	-0.00805	0.29261	-1.79699	4.812	-5.31034	1.9898
	$x > 1.125$	-0.29222	0.68732	-0.38933	0.10963	-0.01166	0	0
ρ_0	$x \leq 1.125$	0.16437	0.09541	-0.77778	2.16077	-2.37432	0.86589	0
	$x > 1.125$	1.24039	-2.78125	2.6344	-1.20503	0.27254	-0.02435	0
$1.5\rho_0$	$x \leq 1.125$	0.16901	-0.03369	0.38116	-1.92408	4.44758	-4.51472	1.61273
	$x > 1.125$	0.67832	-1.52577	1.60052	-0.79736	0.19558	-0.01883	0
$2\rho_0$	$x \leq 1.125$	0.22697	0.0085	-0.62447	1.60553	-1.77879	0.66572	0
	$x > 1.125$	1.3686	-3.15732	2.95638	-1.34067	0.30092	-0.02673	0

[1] F.J. Fattoyev, J. Carvajal, W.G. Newton, B.A. Li, Phys. Rev. C 87, 015806 (2013).

[2] C. Y. Tsang, M. B. Tsang, P. Danielewicz, W. G. Lynch, F. J. Fattoyev, Phys.Lett.B796, 1(2019).

[3] Bao-An Li, Phys. Rev. Lett. 88, 192701 (2002).

[4] L.-W. Chen, C. M. Ko, and B.-A. Li, Phys. Rev. Lett. 94, 032701 (2005).

[5] Yingxun Zhang, Min Liu, Chen-Jun Xia, Zhuxia Li, S. K. Biswal, Phys.Rev.C 101, 034303 (2020).

[6] B. P. Abbott. et al., LIGO collaoration, Phys.Rev.Lett.119, 161101 (2017).

[7] B. P. Abbott. et al., LIGO collaoration, Phys.Rev.Lett.121, 161101 (2018).

[8] F.J.Fattoyev, J. Piekarewicz, C. J. Horowitz, Phys.Rev.Lett. 120, 172702 (2018).

[9] Eemeli Annala, Tyler Gorda, Aleksi Kurkela, and Aleksi Vuorinen, Phys.Rev.Lett. 120, 172703 (2018).

[10] B. P. Abbott. et al., LIGO collaoration, Phys.Rev.X. 9, 011001 (2019).

[11] N.B. Zhang, B. A. Li, J. Xu, Euro.Phys.Jour.A 55, 39 (2019).

[12] Wen-Jie Xie, Bao-An Li, Astrophys. J. 883, 174 (2019).

[13] M.B. Tsang, W. G. Lynch, P. Danielewicz, C. Y. Tsang, Phys.Lett.B 795, 533(2019).

[14] P. Russotto, P.Z. Wu, M. Zoric, M. Chartier, Y. Leifels, R.C. Lemmon, Q. Li, J. Lukasik, A. Pagano, P. Pawłowski, W. Trautmann, Phys. Lett. B 697, 471 (2011).

[15] A. Pagano, P. Pawłowski, W. Trautmann, Phys. Lett. B 697, 471 (2011).

[16] M. Sako, T. Murakami, Y. Nakai, Y. Ichikawa, K. Ieki, S. Imajo, T. Isobe, M. Matsushita, J. Murata, S. Nishimura, H. Sakurai, R.D. Sameshima, E. Takada, arXiv:1409.3322v1 (2014).

[17] W. Reisdorf, M. Stockmeier, A. Andronic, M. L. Ben-abderrahmane, O. N. Hartmann, N. Herrmann, K. D. Hildenbrand, Y. Kim, M. Kiš, P. Koczoń, T. Kress, Y. Leifels, X. Lopez, M. Merschmeyer, A. Schüttauf, V. Barret, Z. Basrakc, N. Bastid, R. Čaplar, P. Crochet, P. Dupieux, M. Dželalija, Z. Fodor, Y. Grishkin, B. Hongf, T.I. Kangf, J. Kecskemeti, M. Kirejczyk, M. Korolija, R. Kottei, A. Lebedeve, T. Matulewicz h, W. Neubert, M. Petrovici, F. Rami k, M.S. Ryuf, Z. Seres, B. Sikora, K.S. Sim, V. Simion, K. Siwek-Wilczyńska, V. Smolyankin, G. Stoiceaj, Z. Tymiński, K. Wiśniewski, D. Wohlfarth, Z.G. Xiao, H.S. Xu, I. Yushmanov, A. Zhilin, Nucl. Phys. A 781, 459 (2007).

[18] Zhigang Xiao, Bao-An Li, Lie-Wen Chen, Gao-Chan Yong, and Ming Zhang, Phys. Rev. Lett. 102, 062502 (2009).

[19] Zhao-Qing Feng, Gen-Ming Jin, Phys. Lett. B 683, 140 (2010).

[20] Wen-Jie Xie, Jun Su, Long Zhu, Feng-Shou Zhang, Phys. Lett. B 718, 1510 (2013).

[21] J. Hong and P. Danielewicz, Phys. Rev. C 90, 024605 (2014).

[22] T. Song and C. M. Ko, Phys. Rev. C 91, 014901 (2015).

[23] M. D. CozmaPhys. Rev. C 95, 014601 (2017).

[24] M.B. Tsang, J. Estee, H. Setiawan, W. G. Lynch, J. Barney, et al, Phys. Rev. C 95, 044614 (2017).

[25] L. Xiong, C. M. Ko, and V. Koch, Phys. Rev. C 47, 788 (1993).

[26] O. Buss, T. Gaitanos, K. Gallmeister, H. van Hees, M. Kaskulov, O. Lalakulich, A. B. Larionov, T. Leitner, J. Weil, and U. Mosel, Phys. Rep. 512, 1 (2012).

[27] W. M. Guo, G. C. Yong, H. Liu, and W. Zuo, Phys. Rev. C 91, 054616 (2015).

[28] Z. Q. Feng, Phys. Rev. C 94, 054617 (2016).

[29] Yangyang Liu, Yongjia Wang, Qingfeng Li, and Ling Liu, Phys. Rev. C 97, 034602 (2018).

[30] Akira Ono, Jun Xu, Maria Colonna, Paweł Danielewicz, Che Ming Ko, Manyee Betty Tsang, Yong-Jia Wang, Hermann Wolter, Ying-Xun Zhang, Lie-Wen Chen, Dan Cozma, Hannah Elfner, Zhao-Qing Feng, Natsumi Ikeno, Bao-An Li, Swagata Mallik, Yasushi Nara, Tatsuhiko Ogawa, Akira Ohnishi, Dmytro Oliynychenko, Jun Su, Taesoo Song, Feng-Shou Zhang, and Zhen Zhang, Phys.Rev.C 100, 044617(2019).

[31] Mao, L. Neise, H. Stöcker, and W. Greiner, Phys. Rev. C 59, 1674 (1999).

[32] N. Kaiser and W. Weise, Phys. Lett. B512, 283 (2001).

[33] L. Girlanda, A. Rusetsky and W. Weise, Nucl. Phys. A 755, 653c (2005).

[34] V. Dmitriev, O. Sushkov, C. Gaarde, Nucl. Phys. A 438, 697 (1985).

[35] Qingfeng Li and Zhuxia Li, arXiv:1712.02062 [nucl-th] (2017).

[36] Zhen Zhang, Che Ming Ko, Phys. Rev. C 95, 064604

(2017).

[37] Ying Cui, Yingxun Zhang, Zhuxia Li, Phys.Rev.C. 98,054605 (2018).

[38] R. Machleidt, K. Holinde, and C. Elster, Phys. Rep. 149, 1 (1987).

[39] M. Benmerrouche, R. M. Davidson, and N. C. Mukhopadhyay, Phys. Rev. C 39, 2339 (1989).

[40] S. Huber and J. Aichelin, Nucl. Phys. **A**573, 587 (1994).

[41] Ying Cui, Yingxun Zhang, Zhuxia Li, Chin. Phys. Rev. C.43, 024105 (2019).

[42] Torleif Ericson and Wolfram Weise, pions and nuclei, (Clarendon press, Oxford, 1988)

[43] L.H. Xia, C.M. Ko, L. Xiong and J.Q. Wu, Nucl. Phys. A 485, 721 (1988) .

[44] G. Baym and S. A. Chin, Nucl. Phys. **A** 262, 527 (1976).

[45] B. Liu, V. Greco, V. Baran, M. Colonna, M. Di Toro, Phys. Rev. C 65, 045201 (2002).

[46] A. Larionov and U. Mosel, Nucl. Phys. **A**728, 135 (2003).

[47] Particle Data Group 2018, <http://pdg.lbl.gov/>.